

## Detection of the effect of nanoparticle preconditioning in a mouse model of prostate cancer by MRI

Isabelle Iltis<sup>1</sup>, Jeunghwan Choi<sup>2</sup>, Manda Vollmers<sup>1</sup>, Mithun Shenoi<sup>2</sup>, John Bischof<sup>2</sup>, and Gregory J Metzger<sup>1</sup>

<sup>1</sup>Radiology, Center for Magnetic Resonance Research - University of Minnesota, Minneapolis, Minnesota, United States, <sup>2</sup>Department of Mechanical Engineering, Bioheat and Mass Transfer Laboratory - University of Minnesota, Minneapolis, Minnesota, United States

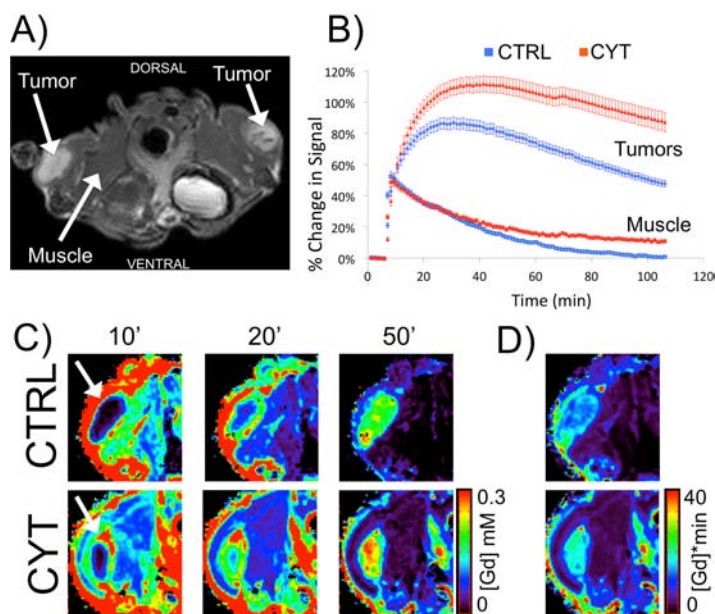
**Introduction.** Cancer therapy efficacy and outcome can be greatly improved when preceded by gold-TNF-alpha nanoparticles administration to “precondition” the tumor. Using destructive, invasive methods in mice models, it has been shown that a drop in perfusion (~80%) and an increase in the interstitial space in the tumor participate in preconditioning [1]. To be clinically relevant, a measurement method compatible with translational studies in human subjects is highly desirable. We recently showed that the effect of a TNF-alpha gold conjugate, CYT-6091, was measurable in a murine model using Dynamic-Contrast Enhanced MRI (DCE-MRI). However, these initial studies were performed using intraperitoneal (IP) injections of contrast agent, since repeated intravenous (IV) injections (e.g. nanoparticle and contrast) into the caudal vein of the mouse are experimentally challenging. To achieve an improved understanding of contrast dynamics relevant to future clinical applications, IV injections were desired to parallel conditions of DCE-MRI in humans. In this work, we show the dynamic characteristics of contrast enhancement after IV delivery of both CYT-6091 and contrast agent in a mouse model of prostate cancer using a jugular vein catheter.

**Materials and Methods.** Ten male nude mice received LnCap cells on both hindlimbs. Four to 5 weeks after implantation, animals were scanned. Mice were divided into 2 groups, one receiving CYT-6091 intravenously via an implanted jugular vein catheter (CYT, n=5) and one control group (CTRL, n=5). Animals receiving CYT were scanned 4 hours after CYT injection. For DCE, gadolinium-DTPA (Gd, 0.1M, 0.3 mmol/kg) was injected intravenously via the jugular vein catheter. Animals were scanned under isoflurane anesthesia using an RF volume coil (Millipede, Agilent, Palo Alto) at a 9.4T magnet equipped with a Varian console. Temperature and respiration rate were monitored throughout the experiment. A multi-slice gradient echo sequence was acquired at multiple flip angles (from 2 to 40°) to calculate T<sub>1</sub> maps prior to contrast agent injection (FOV = 35 mm, matrix size = 128 x 128, 1 mm thickness, TE = 1.43 ms, TR = 65 ms, 4 averages, acquisition time 40s). The same sequence was used to acquire DCE-MRI data to follow contrast kinetics with the following parameter changes (8 averages, FA = 30°, temporal resolution 67 s, total acquisition time = 1h 29min). Enhancement curves were obtained in regions of interest (tumor and muscle) using an open source DICOM viewing software (OsiriX)[2]. Parametric maps were obtained by first converting the signal changes to concentration using standard methods using the pre-contrast T<sub>1</sub> maps [3, 4]. The area under the gadolinium concentration curve (AUGC) was determined by integrating over the 90 minutes of the experiment.

**Results.** Figure 1 shows an axial image of a mouse after Gd injection (A), the percent change in signal after Gd injection in CYT and control mice (B), the concentration maps in one representative animal of each group at different time points (C) and the corresponding AUGC maps (D). In tumors, initial contrast uptake was higher (~40%) and faster in CYT vs. CTRL (as evidenced by the curves and concentration maps at 20') with a slower washout. In the muscle, the initial uptake was comparable, but the enhancement remained ~15% higher over the duration of the experiment in CYT vs CTRL, primarily due to a slower washout.

Figure 1. A) Axial view of a mouse after gadolinium injection. B) Signal enhancement curves obtained in tumors and in the muscle, with (red) or without (blue) CYT treatment. (n=5 in each group). Data are mean ± SEM. C) Concentration maps in CTRL and CYT mice at different time points. D) AUGC maps in CTRL and CYT mice. (Close-ups around the tumor region, indicated by the arrow in C).

Figure 1. A) Axial view of a mouse after gadolinium injection. B) Signal enhancement curves obtained in tumors and in the muscle, with (red) or without (blue) CYT treatment. (n=5 in each group). Data are mean ± SEM. C) Concentration maps in CTRL and CYT mice at different time points. D) AUGC maps in CTRL and CYT mice. (Close-ups around the tumor region, indicated by the arrow in C).



**Discussion/Conclusion.** The interpretation of data obtained following IP contrast injection in previous studies was complicated due to the slower, more diffuse input function. While similar to our previous findings using IP injections, the washin and washout enhancement characteristics were greatly accelerated as expected when injecting the contrast intravenously. By using a jugular vein catheter, DCE-MRI could be successfully used to monitor the permeability and retention effects of nanoparticle administration in a mouse model which mimics the administration of contrast most typically used clinically.

Preconditioning defines an ensemble of complex physiological events involving, in particular, a decrease in perfusion and enhanced permeability and retention (“EPR”) [6] and both mechanisms have been suggested to play a major role in the potentiation of conventional cancer therapies. The slower washout observed here after CYT treatment might reflect the enhanced EPR effect of CYT. We also show that although CYT has a measurable systemic effect, it is highly specific to tumor tissue. In conclusion, DCE-MRI is an excellent, non-invasive method to follow the effect of nanoparticle preconditioning, which is important for the evaluation of nanoparticles as they progress toward clinical trials.

**References.** 1. Goel, R., et al., *Mol Cancer Ther*, 2007. 2. Rosset, A., et al., *J Digit Imaging*, 2004. 3. Daldrup, H.E., et al., *Magn Reson Med*, 1998. 4. Deoni, S.C., et al. *Magn Reson Med*, 2005. 5. Pickup, S., et al. *Acad Radiol*, 2003. 6. Shenoi, M.M., et al., *Nanomedicine (Lond)*, 2011. **Acknowledgements.** Funded by NIH P41 EB015894, and AHC Translational Research Grant Program 2009 09-08. We also gratefully acknowledge CytImmune Sciences, Inc. for providing CYT-6091.